Supplemental information

S1. Fluid flow modeling in the sub-continental lithosphere

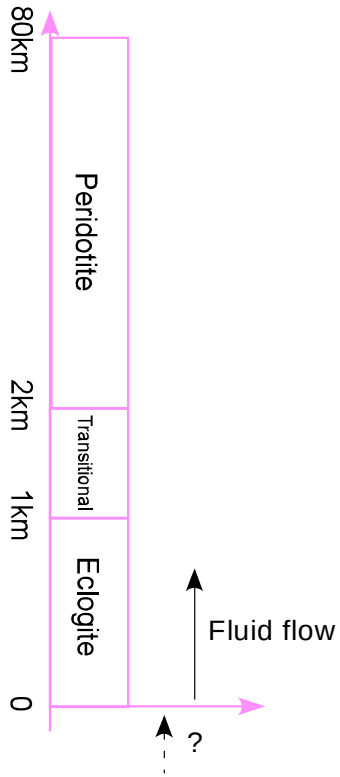

This model is based on Navon and Stolper (1987), assuming C-H-O fluid flows through an upper-mantle peridotite chromatograph, local instant equilibrium, and fluid percolation through an immobile solid. For the sake of simplicity, it ignores diffusion, dispersion, advection, reaction in both solid and fluid phases. In this model, we assume an eclogite block from 0-1km, a transition zone of peridotite from 1-2 km, and a garnet peridotite zone from 2-80 km. In each individual zone and according to mass-conservation laws, the set of governing equation can be written as follows:

$$\begin{cases} \dfrac{\partial C_f}{\partial t} + X_f V_f \dfrac{\partial C_f}{\partial x} = 0 \\ X_f = \dfrac{\phi \rho_f}{\phi \rho_f + (1-\phi)\rho_s D_{Cr}^{Garnet/melt} M_{garnet}} \end{cases}$$

Where C_f represents the concentration of Cr in fluid/melt, ϕ represents porosity, ρ_f is the density of the fluid, ρ_s is the density of the solid, D_{Cr} is the partition coefficient of Cr between garnet and fluid, M_{garnet} is the mode of garnet in rocks (we ignore Cr partitioning in minerals other than garnets), V_f is the velocity of the fluid and $X_f V_f$ is the velocity of the Cr entity which always travels slower than the rate of fluid. In this model, we assume a depth-dependent Cr-partition coefficient:

$$D_{Cr}^{Garnet/melt} = \begin{cases} 8 & 0 < x < 1km \\ 8 + 37*(x-1) & 1km < x < 2km \\ 45 + (15/78)*(x-2) & 2km < x < 80km \end{cases}$$

Initial concentration of the solid is defined as:

$$C_s^{\,0} = \begin{cases} 0.1 & 0 < x < 1\ km \\ 1.8 & 1\ km < x < 2\ km \\ 1.8 & 2\ km < x < 80\ km \end{cases}$$

The boundary conditions include no flux at x = 0 km, allow an out flow at x = 80 km, and continuous at x =1 km and 2 km. Other parameters used are ϕ =0.03, V_f = 80km/year, $M_{peridotite}$=10%, $M_{Eclogite}$=50%, density ratios $\rho_{eclogite}/\rho_{fluid}$ = 1.8 and $\rho_{eclogite}/\rho_{fluid}$ = 1.5. The equations are solved using COMSOL-Multiphysics 4.0. The maximum element size is 10 meters with a growth rate of 1.001. The time step is 10 seconds. Some numerical instability has been smoothed out at the boundaries. Varying the geometry of the each zone, porosity, flow rate, mineral mode and density ratio will not prevent the Cr-spikes in the fluid (generated due to partition coefficient gradient) from propagation, but only vary the time and place where high-Cr garnet could occur. The P-T condition is using the geotherm from Rudnick and Nyblade (1999).

This model requires fluid continuously flushing through peridotite. Since Cr spikes will travel at a much slower speed than the fluid, depending on porosity, density contrast between peridotite

and fluid, mineral mode, and partition coefficient (i.e., the higher the partition coefficient, the slower it moves, see Supplemental information and Navon and Stolper, 1987). The thickness of the 'transitional zone' is limited in the model by the fluid supply. For example, our model moves a Cr-spike over ~ 0.78 km at t = 10^6, but the fluid front has already travelled 2.54 km. The thin transitional zone is consistent with the observation that a narrow range of pressure estimate (38 ± 3 kbar) has been obtained from garnets in garnet peridotite xenoliths from South Africa having Cr_2O_3 = 2-8 % (e.g., Nickel and Green, 1985). A thick 'transitional zone' requires more fluid to flow before high-Cr garnets (e.g., Cr_2O_3 >10%) form. Several mechanisms can expand this zone: 1) fluid coming out of several slabs can move by focused flow; 2) H_2O in the fluid can depress the solidus of mantle peridotites and produce melt; 3) CO_2 formed after the C-H-O fluid is oxidized can further reduce the melting point of mantle peridotites. These fluids will help to produce high-Cr garnets. But diffusion in both fluids and solids will smooth out the sharp boundaries when a 'transitional zone' is thick and flow time is long.

S2. Nature of the high-$\delta^{18}O$ fluid and its relevance to diamond formation

Our study suggests an ^{18}O-enriched fluid component that is related to the formation of high-Cr garnets (maybe diamonds as well), and initially this fluid should be composed of dominantly CH_4 and H_2O with maybe a very small amount of CO_2/CO in order for the generation of reducing-to-oxidizing fO_2 gradient as its reaction with rocks proceeds for the following reasons. First, CO_2 decomposed from carbonate will have high-$\delta^{18}O$ values because modern marine carbonates have $\delta^{18}O_{SMOW}$ = 29‰ and CO_2 in equilibrium with carbonate is ~ 2.0‰ higher than coexisting carbonates at 1200^{o}C (Chacko, et al., 2001). And yet a lower Cr_2O_3 (e.g., <2 wt.%) will be expected as CO_2 flushes through and is reduced by SCLM. Second, although peridotites metasomatized by CH_4 fluid alone will result in a reducing-to-oxidizing fO_2 gradient in SCLM, this process will also produce ^{18}O-depletion in silicate rocks, because $\delta^{18}O$ values of H_2O and CO_2(or CO) as products of chemical reaction between CH_4 and silicates are ~ 2.7 ‰ higher than

coexisting silicates (e.g., $\delta^{18}O_{SMOW}$ = 8.2 ‰ for H_2O and 8.7 ‰ for CO_2 at 1200 ^oC in equilibrium with mantle olivines, Calcite-H_2O, O'Neil, et al., 1969, Forsterite-Calcite, Chiba, et al., 1989, CO_2-Caclcite, Chacko, et al., 1991), leaving ^{18}O-depleted rocks behind. Third, eclogite partial melt will not directly contribute to the formation of high-Cr garnets, because it would react with peridotite at high pressure and freeze at depth (e.g., Yaxley and Green, 1998) and it would not help to generate a partition coefficient gradient. Thus, a significant amount of ^{18}O-enriched H_2O but a small amount of CO_2/CO and melt is allowed in the C-H-O fluids, which favors the formation of diamonds.

Under the framework of this model, the variation of $\delta^{18}O$, Cr content and Mg# in garnets from all-over the world will show the following trends, depending on the chemical and isotopic composition of the fluid and stratigraphic location of rocks (Figs. 6 and 8). Starting from the center of a typical upper mantle range ($\delta^{18}O_{garnet}$ = 5.48 ± 0.17 ‰, Cr_2O_3 = ~2%, Mg# = ~0.82), if the fluid is relatively reduced and ^{18}O-enriched, vector ***a*** ($\delta^{18}O_{garnet}$ increasing with increasing Cr_2O_3 content and Mg#) is expected above the Cr-exchange front, but vector ***b*** ($\delta^{18}O_{garnet}$ increasing with decreasing Cr_2O_3 content and Mg#) below Cr-exchange front (Fig. 7), in which case, all garnets should have $\delta^{18}O_{garnet}$ > 5.48 ‰; If the fluid is relatively oxidized and ^{18}O-enriched, vector ***b*** is expected above the Cr-exchange front but vector ***a*** below Cr-exchange front, in which case, all garnets should have <2% Cr_2O_3, but $\delta^{18}O_{garnet}$ > 5.48 ‰; If the fluid is relatively reduced and ^{18}O-depleted, vector ***d*** (a decreasing $\delta^{18}O_{garnet}$ with decreasing Cr content and Mg#) is expected below the Cr-exchange front but vector ***b*** above Cr-exchange front, in which case, garnets should have $\delta^{18}O_{SMOW}$ values < 5.48 ‰; If the fluid is relatively oxidized and ^{18}O-depleted, vector ***b*** is expected below the Cr-exchange front but vector ***d*** above Cr-exchange front, in which case, garnets should have $\delta^{18}O_{SMOW}$ values < 5.48‰ and Cr_2O_3 content < 2%; vector ***c*** represents decreasing Cr_2O_3 content and Mg# without changing $\delta^{18}O_{garnet}$, this could occur during re-equilibration or melting. The slopes of these vectors rely on the contrast between the fluid and mantle rock and the fluid/rock ratio. These implications will be further tested in the future.

S3. Major element composition

Tables S1 through S5 list major and some minor element compositions of garnets, olivines, clinopyroxenes, orthopyroxenes, serpentines and phlogopite. All measurements are averages of core of 5 mineral grains. Numbers in parentheses represent one standard deviations of least units cited on the basis of replicate analyses. Table S6 presents the raw $\delta^{18}O$ values of silicate minerals from kimberlites.

Table S1. Major element compositions of garnets from Kimberlites

Garnet	SiO_2	TiO_2	Al_2O_3	Cr_2O_3	FeO	MnO	MgO	CaO	Total
UV140/93	41.40(17)	0.07(0)	16.03(10)	10.20(5)	7.00(2)	0.41(2)	21.56(15)	3.18(3)	99.87(47)
BD-794	41.92(45)	0.05(0)	20.81(24)	4.25(3)	6.35(7)	0.32(0)	20.99(11)	4.95(3)	99.65(50)
PHN 2320	41.79(15)	0.06(0)	19.4(15)3	5.90(2)	6.50(3)	0.34(1)	20.49(9)	5.41(4)	99.93(30)
BU-3	42.09(16)	0.06(0)	20.74(5)	4.17(1)	6.17(4)	0.33(1)	21.24(8)	4.91(6)	99.72(40)
BU-26	42.04(14)	0.04(0)	20.71(11)	4.24(0)	6.82(5)	0.34(0)	20.67(6)	5.18(3)	100.05(12)
BU-34	42.20(7)	0.05(0)	22.53(8)	1.95(8)	8.97(4)	0.48(1)	19.95(6)	4.48(6)	100.61(11)
BU-35	42.24(25)	0.01(0)	22.30(19)	2.38(12)	8.39(4)	0.42(2)	20.55(12)	4.56(3)	100.85(23)
MC-2	42.40(8)	0.00(0)	21.96(6)	3.06(1)	7.13(1)	0.43(1)	20.67(3)	4.85(3)	100.51(6)
KPSA-52	41.83(32)	0.09(0)	20.25(17)	4.55(11)	6.44(2)	0.33(1)	20.98(5)	5.31(6)	99.79(39)
KPSA-53	42.29(13)	0.52(1)	19.78(14)	4.12(10)	7.49(18)	0.29(1)	20.96(21)	4.95(3)	100.41(17)
AJE-165	41.88(20)	0.06(0)	19.77(19)	5.08(4)	6.52(3)	0.33(1)	20.56(11)	5.48(2)	99.68(52)
FRB-348	42.32(24)	0.01(0)	21.35(19)	3.90(3)	7.13(7)	0.35(1)	20.89(14)	5.22(2)	101.18(57)
UWG-2	39.91(9)	0.01(0)	22.75(8)	0.005(5)	22.81(17)	0.544(4)	10.89(10)	3.938(3)	100.88(17)

Table S2. Major element compositions of olivines from Kimberlites

Sample	SiO_2	Cr_2O_3	FeO	MnO	NiO	MgO	CaO	Total
UV140/93	41.93(21)	0.04(1)	6.96(2)	0.09(1)	0.37(1)	51.94(43)	0.00(0)	101.34(60)
BD-794	41.41(14)	0.03(1)	7.52(7(	0.09(1)	0.39(1)	51.54(16)	0.02(0)	101.02(19)
PHN 2320	41.52(14)	0.03(1)	7.08(5)	0.08(0)	0.41(1)	51.36(4)	0.01(0)	100.51(15)
BU-3	41.72(12)	0.02	6.67(8)	0.08(1)	0.39(1)	51.93(20)	0.02(0)	100.83(39)
BU-26	41.66(8)	0.02(0)	7.41(4)	0.09(1)	0.40(0)	51.60(16)	0.02(0)	101.21(24)
BU-34	41.26(14)	0.01(1)	9.40(14)	0.11(2)	0.36(3)	50.22(44)	0.02(1)	101.38(23)
BU-35	41.31(12)	0.01(0)	8.34(8)	0.10(1)	0.41(1)	51.36(20)	0.01(0)	101.54(25)
MC-2	41.78(14)	0.01(0)	6.74(5)	0.09(0)	0.41(1)	52.32(9)	0.01(0)	101.38(13)
KPSA-52	41.16(15)	0.05(1)	6.95(9)	0.08(1)	0.40(1)	52.04(15)	0.03(1)	100.71(31)
KPSA-53	40.93(10)	0.05(1)	10.41(10)	0.12(1)	0.35(1)	49.26(17)	0.06(1)	101.23(14)
AJE-165	41.39(4)	0.03(1)	7.08(3)	0.09(0)	0.39(2)	51.11(18)	0.02(0)	100.12(19)
FRB-348	41.39(7)	0.02(0)	7.51(4)	0.09(0)	0.41(1)	51.31(13)	0.02(0)	100.76(15)

Table S3. Major element compositions of orthopyroxenes from Kimberlites

Sample	SiO_2	Al_2O_3	Cr_2O_3	FeO	MnO	NiO	MgO	CaO	Na_2O	Total
BD-794	57.67(16)	1.02(2)	0.39(1)	4.56(1)	0.10(0)	0.11(1)	35.70(15)	0.54(4)	0.13(1)	100.21(15)
PHN 2320	57.95(5)	0.83(2)	0.39(3)	4.43(4)	0.10(1)	0.10(0)	35.85(14)	0.45(0)	0.16(2)	100.28(18)
BU-34	57.81(4)	0.74(3)	0.19(2)	5.57(4)	0.12(1)	0.09(1)	35.51(8)	0.25(2)	0.05(2)	100.37(20)
BU-35	58.47(7)	0.78(2)	0.22(2)	5.20(2)	0.10(0)	0.10(0)	36.43(7)	0.26(2)	0.04(0)	101.61(50)
MC-2	58.23(9)	0.88(2)	0.25(1)	4.30(1)	0.10(0)	0.09(0)	36.43(6)	0.22(1)	0.04(0)	100.54(23)
KPSA-52	58.23(10)	0.79(2)	0.35(1)	4.29(2)	0.11(1)	0.11(1)	36.35(9)	0.46(3)	0.07(1)	100.80(14)
KPSA-53	57.86(5)	1.10(2)	0.29(1)	6.32(1)	0.13(1)	0.11(1)	33.69(5)	1.05(5)	0.33(5)	101.07(35)
FRB-348	58.08(4)	0.74(1)	0.27(1)	4.70(2)	0.11(1)	0.11(1)	35.55(6)	0.45(2)	0.07(1)	100.08(14)

Table S4. Major element compositions of clinopyroxenes from Kimberlites

Sample	SiO_2	TiO_2	Al_2O_3	Cr_2O_3	FeO	MnO	NiO	MgO	CaO	Na_2O	Total
BD-794	54.79(8)	0.10(3)	2.64(20)	1.89(18)	2.12(3)	0.08(0)	0.05(1)	16.85(20)	19.11(40)	2.11(23)	99.74(17)
BU-3	55.04(13)	0.05(0)	2.81(4)	2.07(12)	2.12(3)	0.07(1)	0.05(1)	16.27(13)	18.99(8)	2.45(10)	99.91(13)
BU-26	54.55(10)	0.02(0)	1.72(2)	1.53(10)	2.09(1)	0.07(0)	0.05(1)	17.26(12)	20.79(10)	1.54(8)	99.61(12)
BU-34	54.48(11)	0.10(0)	2.25(3)	1.49(3)	2.58(1)	0.07(1)	0.04(1)	16.00(13)	20.90(8)	1.94(3)	99.85(20)
BU-35	54.52(9)	0.19(2)	1.90(1)	1.56(5)	2.61(2)	0.07(0)	0.04(1)	16.25(15)	21.88(9)	1.60(8)	100.62(30)
MC-2	54.60(8)	0.11(1)	2.93(3)	1.34(2)	2.13(1)	0.09(0)	0.03(1)	16.70(10)	20.56(10)	1.73(7)	100.22(22)
KPSA-52	54.00(10)	0.29(3)	2.64(2)	1.17(1)	2.56(2)	0.11(1)	0.04(1)	17.13(8)	20.82(8)	1.35(5)	100.11(11)
KPSA-53	54.81(9)	0.62(4)	4.15(4)	1.56(3)	4.23(1)	0.12(1)	0.05(1)	17.54(12)	14.83(7)	2.76(6)	100.68(10)

Table S5. Major element compositions of serpentines and phlogopites from Kimberlites

	SiO_2	TiO_2	Al_2O_3	Cr_2O_3	FeO	MnO	NiO	MgO	(OH)	Na_2O	Total
Serpentine											
BU-34	38.3(2.5)		0.19(37)	0.02(1)	7.5(2.1)	0.09(4)	0.16(15)	37.7(1.7)	16.0(1.8)		100
AJE-165	42(4)		0.02(1)	0.02(1)	5.6(1.0)	0.09(0)	0.36(6)	38.0(1.6)	13.8(1.6)		100
Phlogopite											
BU-34	40.87(12)	0.43(0)	13.73(2)	0.75(1)	3.20(3)	0.02(1)	0.21(1)	24.95(9)	5.74(20)	0.71(1)	100

Note: (OH) content is estimated based on the difference of total from 100.

Table S6. Oxygen isotope compositions of coexisting minerals in garnet peridotite xenoliths from South Africa, Tanzania and Siberia

Sample Name	Location	Garnet(‰)	Olivine(‰)	Serpentine(‰)	OPX(‰)	Phlogopite(‰)
UV 140/93[a]	Udachnaya, Siberia	5.04, 5.10	5.40, 5.47	6.88, 6.58		
BD-794	Lashaine, Tanzania	5.24, 5.27	5.28, 5.23		5.72, 5.82	
PHN 2302	Liqhobong, South Africa		5.11, 5.17		5.48, 5.60	
BU-3	Bultfontein, South Africa	5.08,5.15	5.07, 5.12			
Bu-26	Bultfontein	5.06,5.10	5.14, 5.08			
BU-34	Bultfontein	5.28.5.30	5.08, 5.03	5.55, 5.50, 5.57		
BU-35	Bultfontein	5.25,5.27	5.11, 5.01	5.46, 5.57		5.97, 6.07
MC-2	Bultfontein	5.37,5.41	5.25, 5.17	6.24, 5.18, 4.49, 4.29	5.86, 5.91	5.79, 5.85
KPSA-52	Bultfontein	5.07, 5.12	5.01, 5.07	4.80, 5.35	5.76, 5.83	
KPSA-53	Bultfontein	5.10, 5.16	5.14, 5.19	4.94, 5.05		
AJE-165	Bultfontein	5.15,5.19	5.21, 5.13			
FRB-348	Bultfontein	5.30,5.32	5.29, 5.26	5.52, 4.39, 5.72	5.71. 5.77	

All $\delta^{18}O$ values are relative to VSMOW.

Reference:

Chacko, T., Mayeda, T. K., Clayton, R. A. and Goldsmith, J. R. (1991) Oxygen and carbon isotope fractionation between CO2 and calcite. Geochimica Et Cosmochimica Acta **60**, 2595-2608.

Chacko, T., Cole, D. R. and Horita, J. (2001) Equilibrium Oxygen, Hydrogen and Carbon Isotope Fractionation Factors Applicable to Geologic Systems. Reviews in Mineralogy and Geochemistry **43**, 1-81.

Chiba, C.-H., Chacko, T., Clayton, R. N. and Goldsmith, J. R. (1989) Oxygen isotope fractionations involving diopside, forsterite, magnetitem and calcite: Application to geothermometry. Geochimica Et Cosmochimica Acta **53**, 2985-2995.

Navon, O. and Stolper, E. (1987) Geochemical consequences of melt percolation: The upper Mantle as a chromatographic column. The Journal of Geology **95**, 285-307.

Nickel, K. G. and Green, D. H. (1985) Empirical geothermobarometry for garnet peridotites and implications for the nature of the lithosphere, kimberlites and diamonds. Earth and Planetary Science Letters **73**, 158-170.

O'Neil, J. R., Clayton, R. A. and Mayeda, T. K. (1969) Oxygen isotope fractionation in divalent metal carbonates. J. Chem. Phys. **51**, 5547-5558.

Rudnick, R. L. and Nyblade, A. A. (1999) The thickness and heat production of Archean lithosphere: constraints from xenoliths thermobarometry and surface heat flow. In: Fei, Y.-W., Bertka, C.M. and Mysen, B.O. (Ed.), Mantle Petrology: Field Observations and High-Pressure Experimentation: A Tribute to Francis R. (Joe) Boyd, 3-12.

Yaxley, G. M. and Green, D. H. (1998) Reactions between eclogite and peridotite: mantle refertilisation by subduction of oceanic crust. Schweiz. Mineral. Petrogr. Mitt **78**, 243-255.